PROCEEDINGS OF SCIENCE

Results from the LHCf Run II in proton-proton collisions at $\sqrt{s}$ = 13 TeV

A. Tiberio,[a,*] **O. Adriani,**[a,b] **E. Berti,**[a,b] **L. Bonechi,**[a] **M. Bongi,**[a,b] **R. D'Alessandro,**[a,b] **G. Castellini,**[c] **M. Haguenauer,**[d] **Y. Itow,**[e,f] **K. Kasahara,**[g] **M. Kondo,**[e] **Y. Matsubara,**[e] **H. Menjo,**[e] **Y. Muraki,**[e] **K. Ohashi,**[e] **P. Papini,**[a] **S. Ricciarini,**[a,c] **T. Sako,**[h] **N. Sakurai,**[i] **K. Sato,**[e] **Y. Shimizu,**[j] **T. Tamura,**[k] **S. Torii,**[k] **A. Tricomi,**[l,m,n] **W. C. Turner,**[o] **M. Ueno**[e] **and K. Yoshida**[g]

[a] *INFN Section of Florence, Florence, Italy*
[b] *University of Florence, Florence, Italy*
[c] *IFAC-CNR, Florence, Italy*
[d] *Ecole-Polytechnique, Palaiseau, France*
[e] *Institute for Space-Earth Environmental Research, Furo-cho, Chikusa-ku, Nagoya, Japan*
[f] *Kobayashi-Maskawa Institute for the Origin of Particles and the Universe, Nagoya University, Nagoya, Japan*
[g] *Faculty of System Engineering, Shibaura Institute of Technology, Tokyo, Japan*
[h] *Institute for Cosmic Ray Research, University of Tokyo, Chiba, Japan*
[i] *Tokushima University, Tokushima, Japan*
[j] *Kanagawa University, Kanagawa, Japan*
[k] *RISE, Waseda University, Shinjuku, Tokyo, Japan*
[l] *INFN Section of Catania, Catania, Italy*
[m] *University of Catania, Catania, Italy*
[n] *CSFNSM, Catania, Italy*
[o] *LBNL, Berkeley, California, USA*

E-mail: alessio.tiberio@fi.infn.it

[*] Speaker

© Copyright owned by the author(s) under the terms of the Creative Commons Attribution-NonCommercial-NoDerivatives 4.0 International License (CC BY-NC-ND 4.0).

PoS(EPS-HEP2021)105

The LHCf experiment, at the Large Hadron Collider (LHC), consists of two small independent calorimeters placed 140 metres away, on opposite sides of the ATLAS interaction point (IP1). LHCf has the capability to measure zero-degree neutral particles, covering the pseudorapidity region above 8.4. By measuring the very-forward particle production rates at the highest energy possible at an accelerator, LHCf aims to improve our understanding of hadronic interactions in air-showers induced by ultra-high-energy cosmic rays in the atmosphere. This contribution will highlight recent results from Run II measurements with p-p collisions at 13 TeV. At first, the advantages of an ATLAS-LHCf combined analysis are discussed and a preliminary energy spectrum of very-forward photons produced in diffractive collisions as tagged by ATLAS is shown. The neutron energy spectrum measurements, for several pseudorapidity regions, are presented and compared with the predictions of various hadronic interaction models. From these measurements the average inelasticity of the collisions, which strongly affects the development of an air-shower, has also been extracted. Finally, the preliminary π^0 Feynman-x and transverse momentum spectra, which affect the development of the electromagnetic component of an air-shower, are shown.

PoS(EPS-HEP2021)105

**** The European Physical Society Conference on High Energy Physics (EPS-HEP2021), ****
**** 26-30 July 2021 ****
**** Online conference, jointly organized by Universität Hamburg and the research center DESY ****

1. Introduction

The indirect detection techniques of the Ultra-High-Energy Cosmic Rays (UHECRs, with energies $\gtrapprox 10^{18}$ eV) are based on the observation of the shower of secondary particles produced in the interaction of a cosmic ray with a nucleus of the atmosphere (the so-called "air-showers"). A clear interpretation of the data of ground based experiments is made difficult due to the large systematic uncertainty associated to the disagreement between different hadronic interaction models employed in the simulations of the air-showers. The tuning of these phenomenological models with experimental data is therefore fundamental to reduce the systematic uncertainty of UHECR measurements. The LHC-forward (LHCf [1]) experiment is designed to measure the very-forward neutral particles production at the Large Hadron Collider (LHC). The very-forward region covered by LHCf is crucial for the tuning of hadronic interaction models since it is the region where most of the energy flow of secondary particles is contained. After a brief description of the experimental apparatus in Section 2, the LHCf analysis results for photon, neutron and π^0 production in proton-proton collisions at $\sqrt{s}$ = 13 TeV will be presented in Section 3.

2. The LHCf experiment

The LHCf experiment is composed of two independent detectors (named "Arm1" and "Arm2") placed ~140 meters away from the Interaction Point 1: The detectors are placed in the Target Absorber Neutral (TAN) instrumentation slot, where the beam pipe from the interaction point turns into two separate beam pipes: this position allows the measurement of particles emitted at a pseudorapidity $\gtrsim$ 8.4, up to zero-degree. Since charged particles are deflected by the dipole magnets which bend the colliding beams into their own beam pipes, only neutral particles can be measured by the detectors. Each detector is made of two sampling and position sensitive calorimeters (called "towers" hereafter) which use Gd_2SiO_5 (GSO) scintillators as active layers and tungsten as absorber. Each tower contains 4 couples of position sensitive layers to measure the transverse position: GSO scintillator bars are used in Arm1 while silicon microstrip detectors are used in Arm2. All calorimeters have a depth of 44 radiation lengths and 1.6 hadronic interaction lengths. The energy resolution is better than 3% for photons above 100 GeV [2] and ~40% for neutrons. The position resolution of the silicon microstrip detectors for electromagnetic showers is 40μm [3], while for GSO bars is 200 μm [2]. Position resolution for neutrons showers is ~1 mm.

3. LHCf Run II results

The data set used in the following analyses has been taken during the LHCf operation in proton-proton collisions at $\sqrt{s}$ = 13 TeV in LHC fill #3855. A dedicated low-luminosity beam setup was used with a luminosity of $0.4 \div 1.4 \times 10^{29}$ cm^{-2} s^{-1}. The photon and neutron analysis results shown in Section 3.1 and 3.2 used an integrated luminosity of 0.19 nb^{-1}, while the π^0 analysis used a larger data sample of 2.1 nb^{-1} and 0.8 nb^{-1} for Type I and Type II π^0 events, respectively (see Section 3.3 for the explanation of the event types).

PoS(EPS-HEP2021)105

3.1 LHCf-ATLAS combined photon analysis

LHCf photon measurements in p-p collisions at 13 TeV have already been published [4]. However, the LHCf experiment alone does not have the capability to distinguish the type of collision occurred at the interaction point. Since 2013 LHCf and ATLAS [5] experiments exchange the trigger signals during LHCf dedicated runs, so it is possible to perform a combined analysis with the event information from both experiments. The number of tracks recorded by ATLAS detectors in the central region can be used to discriminate diffractive events from non-diffractive ones: selecting events with no charged particles in the region $|\eta| < 2.5$ a pure sample of low-mass ($M_X < 20$ GeV) diffraction events can be selected [6]. The preliminary results of the combined analysis are presented in Figure 1 [7], where the photon energy spectrum is shown for both the inclusive and the low-mass diffraction component. The diffraction spectrum of EPOS model has a good agreement with data in the $\eta > 10.94$ region, while PYTHIA model has a better agreement for $8.81 < \eta < 8.99$.

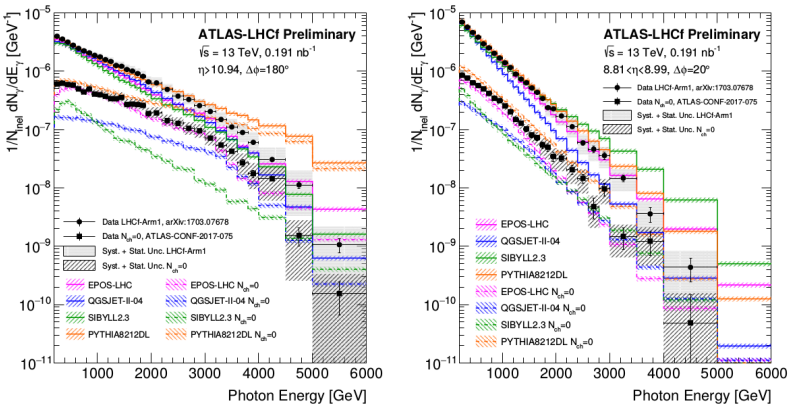

Figure 1: Photon energy spectrum for pseudorapidity regions $\eta > 10.94$ (left) and $8.81 < \eta < 8.99$ (right) in p-p collisions at $\sqrt{s}$ = 13 TeV. Measured inclusive and low-mass diffractive spectra are represented as black circles and squares, respectively. Predictions from several hadronic interaction models for the inclusive and diffractive spectra are represented as solid and dashed lines, respectively. Hatched areas show statistical+systematic errors for data and statistical errors for simulations.

3.2 Neutron energy spectrum and average inelasticity

The neutron energy spectrum in six pseudorapidity bins is shown in Figure 2 [8]. All the distributions exhibit a peak structure, whose position progressively moves to lower energy as pseudorapidity decreases. As already noted [9], the largest disagreement between LHCf data and hadronic interaction models is found in the most forward region ($\eta > 10.75$): the peak structure of the data is not reproduced by any model and all models underestimate the neutron yield by at least 20%. In the other pseudorapidity regions either SIBYLL or EPOS models have a better agreement with respect to other models. The distribution of the elasticity of the collision ($k_n \equiv 2E_n/\sqrt{s}$, where E_n is the energy of the neutron) is shown in the top panel of Figure 3, while the average inelasticity $(1 - k_n)$ is shown in the bottom panel. Even if no model well reproduces the elasticity distribution, the predicted average inelasticity of all models has a good agreement with the measured one.

PoS(EPS-HEP2021)105

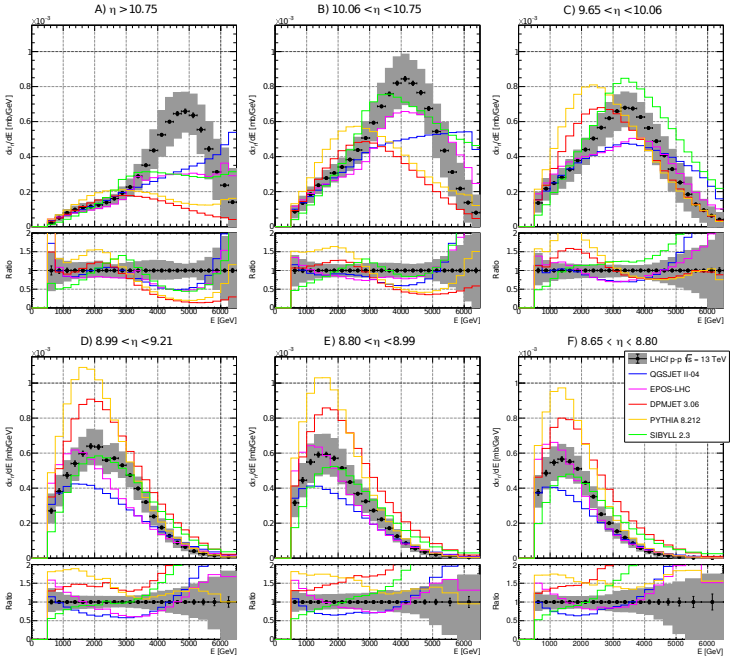

Figure 2: Measured neutron energy spectrum (black points) in different pesudorapidity bins compared with models predictions (coloured histograms). Grey area represents statistical+systematic uncertainty.

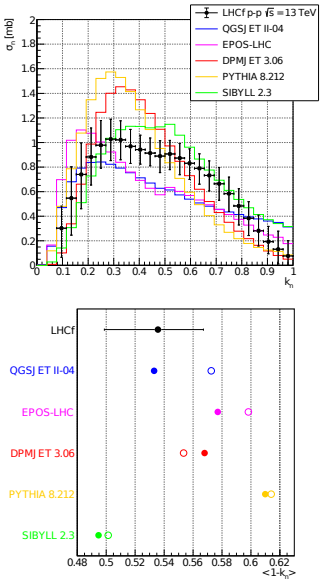

Figure 3: Top: neutron elasticity distribution for data (black points) and models predictions (coloured histograms). Bottom: average inelasticity for neutron events (full circles) and all event (open circles).

3.3 Neutral pion p_T vs X_F spectrum

The π^0 transverse momentum (p_T) and Feynman-X ($X_F \equiv 2p_Z/\sqrt{s}$) are reconstructed from the energy and impact position of the decay photons into the LHCf towers. Two typology of events can be recorded: "Type I" events where one photon hits each tower, and "Type II" events where both photons hit the same tower. The preliminary p_T spectra in several X_F bins are shown in Figure 4. Type I and Type II analyses provide results in good agreement in the regions where they overlap, and Arm1 and Arm2 data also appear to be consistent with each other. The consistency of the data between different detectors and event types permits to fully take advantage of the different p_T and X_F coverage of Arm1 and Arm2, and of Type I and Type II events. Indeed, thanks to the larger dimension of its large tower, Arm1 is able to reach a larger p_T with respect to Arm2. Conversely, Arm2 close the gaps of Arm1 acceptance for $X_F < 0.6$ and extend the low-p_T coverage for $X_F > 0.6$ thanks to the larger dimension of its small tower.

References

[1] O. Adriani, L. Bonechi, M. Bongi, G. Castellini, R. D'Alessandro, D.A. Faus et al., *The LHCf detector at the CERN large hadron collider*, *Journal of Instrumentation* **3** (2008) S08006.

[2] Y. Makino, A. Tiberio, O. Adriani, E. Berti, L. Bonechi, M. Bongi et al., *Performance study*

PoS(EPS-HEP2021)105

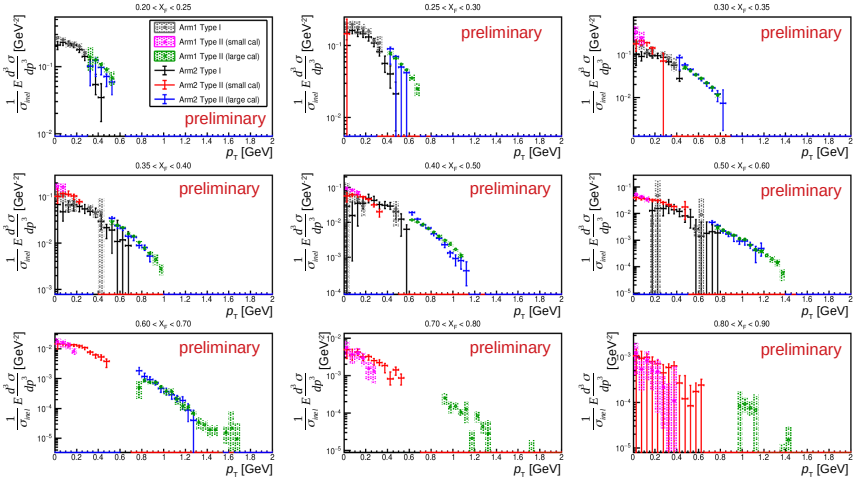

Figure 4: Transverse momentum spectra in different X_F bins measured with the Arm1 and Arm2 detectors of LHCf. Results from different detectors and π^0 event types are shown with different colors. Errors bars represent the total estimated uncertainty (statistical + systematic).

for the photon measurements of the upgraded LHCf calorimeters with Gd_2SiO_5 (GSO) scintillators, *Journal of Instrumentation* **12** (2017) P03023.

[3] O. Adriani, L. Bonechi, M. Bongi, G. Castellini, R. Ciaranfi, R. D'Alessandro et al., *The construction and testing of the silicon position sensitive modules for the LHCf experiment at CERN*, *Journal of Instrumentation* **5** (2010) P01012.

[4] O. Adriani, E. Berti, L. Bonechi, M. Bongi, R. D'Alessandro, M. Haguenauer et al., *Measurement of forward photon production cross-section in proton–proton collisions at $\sqrt{s} = 13$ TeV with the LHCf detector*, *Physics Letters B* **780** (2018) 233.

[5] T.A. Collaboration, G. Aad, E. Abat, J. Abdallah, A.A. Abdelalim, A. Abdesselam et al., *The ATLAS experiment at the CERN large hadron collider*, .

[6] Q.-D. Zhou, Y. Itow, H. Menjo and T. Sako, *Monte Carlo study of particle production in diffractive proton–proton collisions at $\sqrt{s} = 13$ TeV with the very forward detector combined with central information*, *The European Physical Journal C* **77** (2017) 212.

[7] ATLAS Collaboration collaboration, *Measurement of contributions of diffractive processes to forward photon spectra in pp collisions at $\sqrt{s} = 13$ TeV*, *ATLAS-CONF-2017-075* (2017) .

[8] O. Adriani, E. Berti, L. Bonechi, M. Bongi, R. D'Alessandro, S. Detti et al., *Measurement of energy flow, cross section and average inelasticity of forward neutrons produced in $\sqrt{s} = 13$ TeV proton-proton collisions with the LHCf Arm2 detector*, *Journal of High Energy Physics* **2020** (2020) 16.

[9] O. Adriani, E. Berti, L. Bonechi, M. Bongi, R. D'Alessandro, S. Detti et al., *Measurement of inclusive forward neutron production cross section in proton-proton collisions at $\sqrt{s} = 13$ TeV with the LHCf Arm2 detector*, *Journal of High Energy Physics* **2018** (2018) 73.

PoS(EPS-HEP2021)105